South Asian Summer Monsoon and subtropical deserts

K. P. Sooraj, Pascal Terray, Annalisa Cherchi

Chapter 15

South Asian Summer Monsoon and subtropical deserts

Dr. K.P. Sooraj [Centre for Climate Change Research, Indian Institute of Tropical Meteorology, Ministry of Earth Sciences (IITM-MoES), Pune 411008, India]

Dr. Pascal Terray [Sorbonne Universites (UPMC, Univ Paris 06)-CNRS-IRD-MNHN, LOCEAN Laboratory, Paris, France]

Dr. Annalisa Cherchi [Institute of Atmospheric Sciences and Climate (ISAC-CNR), Bologna, Italy; Istituto Nazionale di Geofisica e Vulcanologia, INGV, Bologna, Italy]

Corresponding author address:

Sooraj K. P.

Centre for Climate Change Research, Indian Institute of Tropical Meteorology,

Ministry of Earth Sciences (IITM-MoES)

Pune 411008, India, e-mail:sooraj@tropmet.res.in

Abstract

The relationships between south Asian monsoon and Northern Hemisphere (NH) subtropical deserts have generated a lot of research in the recent times as both systems, despite of contrasting climates, are expected to be severely affected by anthropogenic climate change. This review envisages two pathways for the monsoon-desert relationship. The first one hypothesizes a significant influence of the monsoon on subtropical deserts whereby convection over the Indian Summer Monsoon (ISM) region induces Rossby-wave descent to its west. The second one proposes a very different perspective by emphasizing the potential role of NH deserts on ISM either through the changes of surface heating over the subtropical deserts or by dry air intrusions from arid regions into the monsoon domain. However, most current coupled climate models struggle to simulate realistically these monsoon-desert relationships due to various reasons, as documented in this chapter, calling for advances in coupled models with improved physical parameterizations.

Keywords: Indian summer monsoon, NH subtropical deserts, monsoon-desert relationship, anthropogenic climate change

15.1 Introduction

Monsoon and desert regions coexist at the subtropical latitudes of the African-Asian continent (e.g., Rodwell and Hoskins, 1996; Warner, 2004). The mutual association between these two contrasting climates has been studied in the past as well as in the recent times (e.g., Ramage, 1966; Charney, 1975; Charney et al., 1977; Shukla and Mintz, 1982; Sud and Fennessy, 1982; Smith, 1986a, 1986b; Mooley and Paolino, 1988; Sud et al., 1988; Parthasarathy et al., 1992; Yang et al., 1992; Webster, 1994; Rodwell and Hoskins, 1996, 2001; Sikka, 1997; Claussen, 1997; Bonfils et al., 2000; Douville et al., 2001; Xue et al., 2004; Yasunari et al., 2006; Wang, 2006; Wu et al., 2009; Biasutti et al., 2009; Lavaysse et al., 2009; Xue et al., 2010; Bollasina and Nigam, 2011a, 2011b; Bollasina and Ming, 2013; Tyrlis et al., 2013; Cherchi et al., 2014; Vinoj et al., 2014; Shekhar and Boos, 2017; Sooraj et al., 2019). As desertification is a fundamental process of the ongoing climate change (Cook and Vizy, 2015; Zhou, 2016; Wei et al., 2017) and climate projections of the south Asian monsoon remain uncertain (e.g., IPCC, 2013; Sabeerali et al., 2015; Annamalai et al., 2015; Sooraj et al., 2015; Krishnan et al., 2016; Kitoh, 2017; Singh and Achutarao, 2018; Wang et al., 2020), a renewed interest to understand the monsoon-desert relationships has grown. Furthermore, these two climate systems are affected by severe temperature, rainfall and radiation biases in current climate models (e.g., Bollasina and Ming, 2013; Levine et al., 2013; Sperber et al., 2013; Roehrig et al., 2013; Prodhomme et al., 2014; Sandeep and Ajayamohan, 2015; Samson et al., 2016; Haywood et al., 2016; Terray et al., 2018), and improving their representation is an important aspect to have better climate forecasts and projections (e.g., Cherchi et al., 2014; Terray et al., 2018; Sooraj et al., 2019).

Against the backdrop of this, we made an attempt to provide a comprehensive overview of the mutual relationships between these two contrasting climates thereby highlighting the

underlying mechanisms. The chapter is organized as follows: Section 15.2 describes the salient climatological characteristics of the monsoon-desert system and highlights the historical background on the existence of subtropical deserts over African-Asian regions at the same latitude than the south Asian monsoon. Section 15.3 focuses on the south Asian monsoon (i.e., Indian Summer Monsoon, ISM) influence on the hot subtropical deserts, thus presenting the monsoon-desert paradigm using observation, reanalysis and coupled General Circulation Models (GCMs). Section 15.4 reviews the literature on the potential role of deserts in modulating the ISM. Finally, Section 15.5 encapsulates the main highlights as drawn from this Chapter review.

15.2 The Monsoon-Desert system: Background settings

The monsoon-desert system over African-Asian region is characterised by a sharp rainfall gradient during the boreal summer (e.g., from June to September) with heavy rainfall in the monsoon regions of the northern hemisphere (NH), but only sporadic and low rainfall in the adjacent arid regions (Fig. 15.1a). The contrasts between the two climates are further corroborated when considering other important parameters such as surface albedo or net radiation budget at the Top of the Atmosphere (TOA; Fig. 15.1b-c).

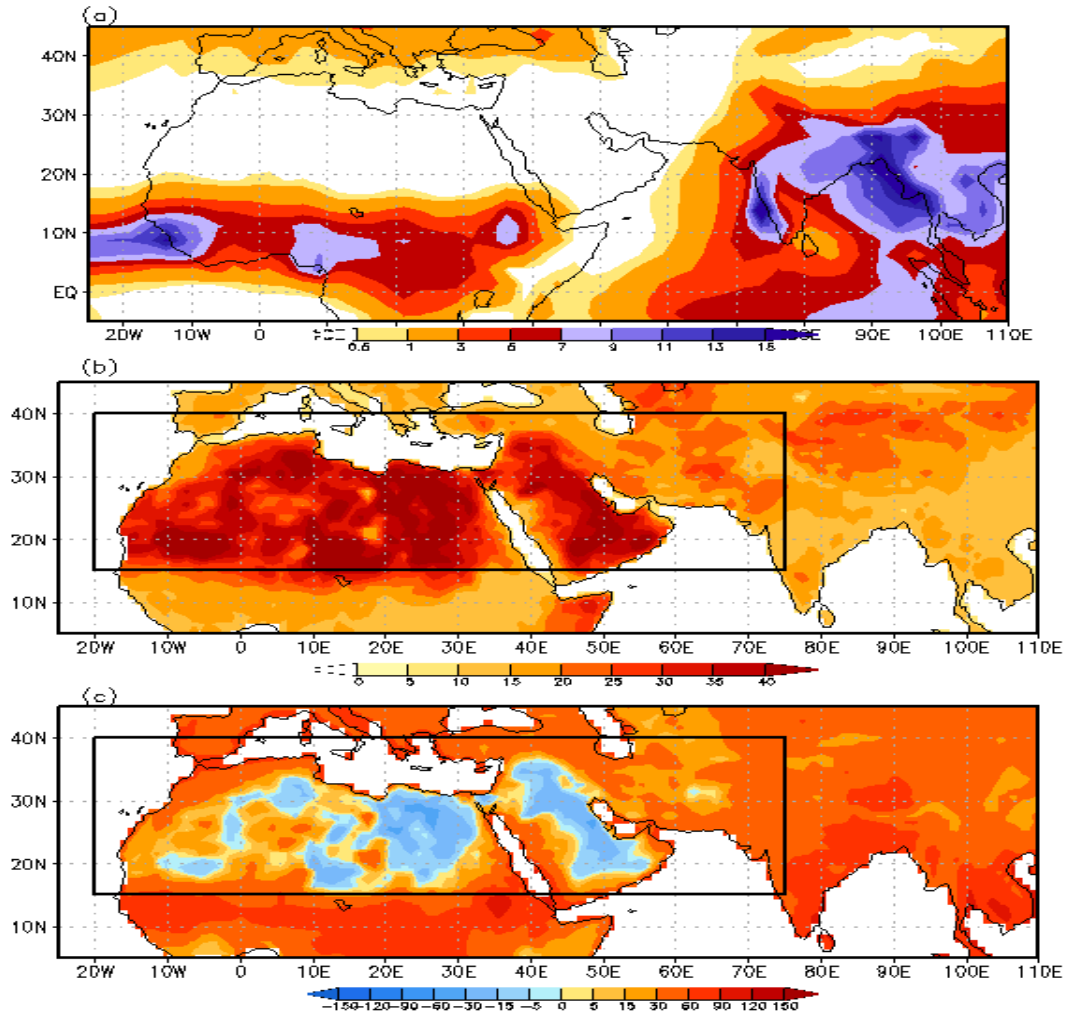

Figure 15.1: Climatological map of (a) rainfall (mm day^{-1}), (b) land surface albedo (%) and (c) net radiation budget at TOA (Wm^{-2}), for boreal summer period (June to September). In (a) rainfall climatology is computed for the 1986-2014 period from Global Precipitation Climatology Project (GPCP version 2.1; Huffman et al., 2009). In (b) and (c), albedo and radiation climatology is computed for the 2000-2018 period from the Clouds and the Earth's Radiant Energy System Energy Balanced and Filled (CERES-EBAF edition 4.0; Kato et al., 2018). In (b) and (c), the region highlighted in the black rectangle refers to "subtropical deserts".

90 The subtropical desert regions, with bright sandy surface terrains, clear sky conditions,
91 high temperature, reduced soil moisture and lack of vegetation, are characterised by relatively
92 high surface albedo (Fig. 15.1b; Sikka, 1997; Warner, 2004; Terray et al., 2018; Sooraj et al.,
93 2019). Figure 15.1b shows two important examples for subtropical deserts: The Arabian-Iran-
94 Thar desert located just to the west of the ISM system (Sikka, 1997) and the Sahara just to the
95 north of the West African Monsoon (WAM) (Lavaysse et al., 2009). In this Chapter, these high
96 albedo regions lying across north Africa and west Asia (i.e., the geographical region bounded by
97 20°W–75°E, 15°–40°N; Fig. 15.1b) are hereafter collectively referred to as "subtropical deserts"
98 (or simply "arid regions").

99 As per the traditional theory dating back to the 1970s, the subtropical desert climates are
100 associated with the descending branch of the Hadley circulation over the subtropics of the NH
101 (Warner, 2004). However, NH Hadley circulation is weakest during boreal summer, which is
102 completely out of synchronization with some of the observed summer climate features along the
103 NH subtropics (e.g., the co-existence of both moist monsoon and desert climates at the same
104 latitude). Consequently, this traditional view is now not well accepted in the literature (Yang et
105 al., 1992; Rodwell and Hoskins, 1996; Wang, 2006; Wu et al., 2009). In a pioneering study,
106 Charney (1975) made an attempt to explain the enhancement of subsidence over subtropical
107 desert of the NH during boreal summer, by invoking a mechanism called biosphere-albedo
108 feedback. As per their study, the pronounced reduction in vegetation cover (i.e., over-grazing)
109 over subtropical deserts regions increases surface albedo, thus causing enhanced radiative
110 cooling (Fig. 15.1c). This radiative loss is balanced by enhanced descent (Fig. 15.2), which in
111 turn results in reduced rainfall, thus leading to further decrease in vegetation cover (i.e.,
112 desertification amplification). However, their mechanism ignored the possible influence of

horizontal heat advection and hence found to be inappropriate over the NH subtropical deserts (e.g., Hoskins, 1986). Later, Yang et al. (1992) and Webster (1994) proposed another concept involving a closed "Walker type" circulation linking convection over south Asia to the subsidence over arid regions to its west. Nevertheless, subsequent studies (i.e., the seminal work of Rodwell and Hoskins, 1996, 2001; Hoskins, 1986) dispelled this notion, as their studies showed no signature of a closed overturning circulation. Based on the scale analysis of the thermodynamic equation, Rodwell and Hoskins (1996) also argued for the importance of horizontal heat advection for the existence of these subtropical desert regions. This currently recognized paradigm is often referred in the literature as the "monsoon-desert mechanism", and is further described in Section 15.3.

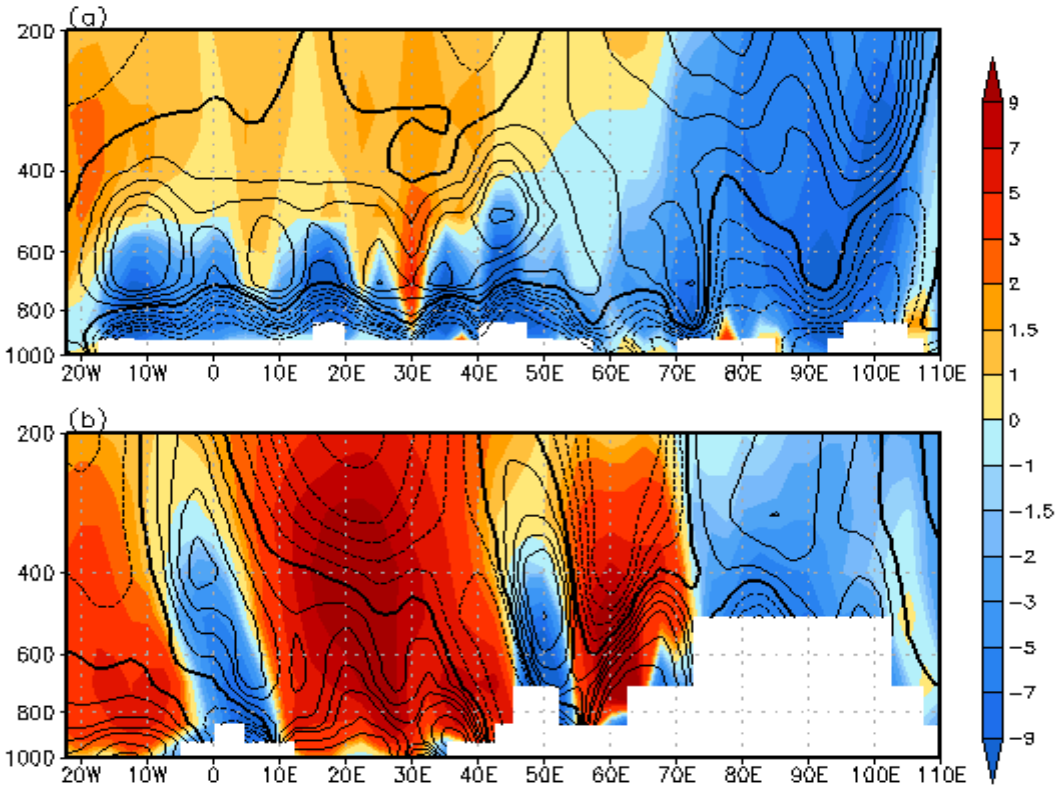

Figure 15.2: Vertical cross-section of atmospheric circulation in terms of vertical component of velocity (10^{-2} Pa s^{-1}, shaded) and horizontal wind divergence (10^{-6} s^{-1}, contours) during July, along a pressure-longitude plane averaged over two latitude bands (a) 20^0N and (b) 40^0N. The circulation fields are taken from the ERA-Interim reanalysis (Dee et al., 2011) and the climatology is computed for the 1986-2014 period. The negative (dashed) and positive (continuous) contours correspond, respectively, to absolute magnitudes of 1, 2, 3 and 4 units. The zero contours are highlighted in thick black color. Negative (positive) shading implies ascending (descending), while negative (positive) contours implies convergence (divergence). The presentation using July climatology follows the observational conjecture that it corresponds to the peak of monsoon activity (e.g., Tyrlis et al., 2013).

In contrast to the subtropical desert, the vegetated land surface over south Asian landmass shows a reduced surface albedo and the ISM region is radiatively surplus highlighting the role of clouds and moisture on the radiation balance (Fig. 15.1b-c; Sooraj et al., 2019). Furthermore, the ISM land region and the Bay of Bengal are characterized by strong ascending motion extending throughout the troposphere (see Fig. 15.2a), thus exemplifying the monsoon induced stratification due to the ISM rainfall and its associated diabatic heating (Fig. 15.1a). The corresponding low-level convergence is consistent with the thermo-dynamical response due to this diabatic heating (Fig. 15.2a; e.g., Neelin and Held, 1987).

The transition zone between this ISM convection center and the hot subtropical deserts to its west (i.e., extending from Mediterranean to west Asian landmass) is characterized by the existence of several regional heat lows with lower-level convergence and ascending motions (i.e., below 600-hPa) capped aloft by upper-level subsidence and divergence (i.e., mostly

148 confined between 200 and 600-hPa) as displayed in Figure 15.2a. Figure 15.2b shows the
149 intensification of these descending motions (extending throughout the troposphere) over west
150 Asia and eastern Mediterranean regions at the northern boundary of the domain, thus
151 highlighting the pronounced subsidence over these regions. Figure 15.2a-b highlights that the
152 southern and northern regions of the hot subtropical deserts show totally different vertical
153 structures of the local atmospheric circulation (Sooraj et al., 2019).

154 **15.3 Monsoon influence over hot subtropical deserts**

155 The idea that the existence of subtropical deserts is related to the ISM is dated back to
156 mid-90s. Rodwell and Hoskins (1996) suggested a monsoon-desert mechanism whereby, in a
157 linear modelling framework, remote diabatic heating in the Asian monsoon region induces a
158 Rossby-wave pattern to the west, interacting with the southern flank of the mid-latitude
159 westerlies and causing descent over eastern Sahara and the Mediterranean (Figs. 15.2 and 15.3).
160 The associated atmospheric response has the form of an anticyclone at upper levels and a
161 cyclone at lower levels, with a deepening of the isentropic surfaces due to the mid-tropospheric
162 warming (Fig. 15.3a). When this far poleward thermal structure interacts with the southern flank
163 of the mid-latitude westerlies, the air moves down the isentropes on their western side (Wang et
164 al., 2012), as evident from Figure 15.3b where the northerly component of the westerly flow
165 crosses the isentropic surfaces. Further, according to Rodwell and Hoskins (1996), the subsiding
166 air is also of mid-latitude origin as revealed by their trajectory analysis. Regions of adiabatic
167 descent are strengthened by "local diabatic enhancement" and longitudinal mountain chains
168 induce a blocking of the westerly flow (Rodwell and Hoskins, 2001). The idea of the monsoon-
169 desert mechanism linking the ISM to the Mediterranean has been then easily extended to other
170 regions with Mediterranean-type of climates, like California and Chile, remotely forced by

monsoon regions to the east (Rodwell and Hoskins, 2001). Overall, the theoretical framework based on these pioneering works is well established in terms of the origin of subtropical highs in the summer hemispheres (Cherchi et al., 2018).

In agreement with idealized model simulations, results focused on ERA40 reanalysis (Uppala et al., 2005) confirmed strong mid and upper-level warming spreading westward and causing significant depression of the isentropes, which are linked to Rossby wave activity away from the diabatic heating sources (Tyrlis et al., 2013). Over the eastern Mediterranean and Middle East, the subsidence and northerly flow (Etesian winds) are recognized as manifestations of the Rossby wave structure triggered by the ISM convection (Tyrlis et al., 2013; Rizou et al., 2018). In a similar framework, processes at work in the monsoon-desert mechanism have been analyzed in 20th century simulations from coupled GCMs participating to the 5th Coupled Model Intercomparison Project (CMIP5; Taylor et al., 2012), showing how few of them are able to simulate the mechanism for the correct reasons (Cherchi et al., 2014). CMIP5 coupled GCMs tend to underestimate (overestimate) ISM related diabatic heating at upper (lower) levels, resulting in a weaker forced response (Cherchi et al., 2014). Moreover, CMIP5 coupled GCMs with a severe dry bias over the ISM region depict the weakest mid-latitude winds and minimum descent over the Mediterranean, as well as little vertical variation in diabatic heating (Cherchi et al., 2014). On the other hand, when simulated precipitation over India improves in the coupled GCMs, the extratropical teleconnection with the Mediterranean region improves as well (Jin et al., 2019). In other words, the uncertainty associated with monsoon simulations needs to be considered in future climate projections even outside the monsoon domain. Interestingly, air-sea coupling seems also to be important to correctly represent the monsoon-desert teleconnections, as in coupled model simulations the divergence field associated with the ISM is more favorable

for inducing westward Rossby wave propagation than in uncoupled simulations (Osso' et al., 2019).

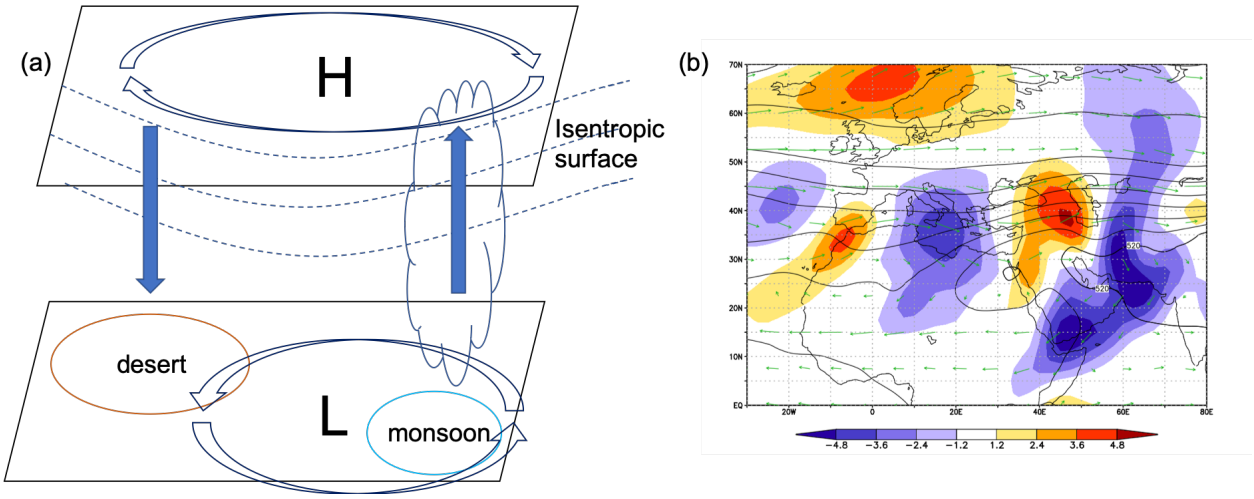

Figure 15.3: (a) Schematic diagram of the monsoon desert-mechanism with descent over the desert region (orange) induced by the heating over the monsoon convective region (cyan) interacting with local westerlies. [Adapted by permission from Wang et al., 2012]. (b) JJA mean wind (ms^{-1}, green vectors), meridional wind velocity (ms^{-1}, shaded), and pressure levels (hPa, contours with 50-hPa contour interval) on isentropic surfaces at 325K using NCEP/NCAR reanalysis dataset (Kalnay et al., 1996). The climatology is computed for the period 1958-2019.

Within boreal summer, descent enhancement over the Mediterranean and east Sahara has been observed during the onset of the ISM (Rodwell and Hoskins, 1996). In early July, when convection migrates over northern continental India, the Rossby wave structure amplifies impacting the circulation over the eastern Mediterranean and Middle East (Tyrlis et al., 2013). In the peak of the monsoon season, the combined diabatic heating pattern over the Arabian Sea and

211 Bay of Bengal regions exerts the largest descent over the eastern Mediterranean (Cherchi et al.,
212 2014). As the monsoon activity is associated with active and break spells, it could be argued that
213 successive Rossby wave pulses are released, inducing a cumulative effect over the region until
214 the peak of the monsoon activity is reached in July (Tyrlis et al., 2013).

215 The processes recognized as part of the monsoon-desert mechanism vary at interannual
216 timescales as well, with imprints of severe weak and strong ISMs noticeable over the
217 Mediterranean (Cherchi et al., 2014). Interestingly, the monsoon forcing is more significant
218 during strong ISMs, with enhanced subsidence over the Mediterranean region, than during weak
219 ISMs (see Fig. 15.4). During a strong monsoon, upper tropospheric heating expands westward
220 reaching a maximum over northern Arabian Peninsula modulating thermodynamic and dynamic
221 patterns there and likely governing the occurrence of extremes over the region (Attada et al.,
222 2019). ISM rainfall is significantly and negatively correlated with precipitation over Black
223 Sea/Balkans region (Osso' et al., 2019). This kind of relationships suggests the possibility of
224 using the ISM characteristics as potential predictors for the summer conditions over the
225 Mediterranean region. At interannual to inter-decadal timescales, these dynamics are part of a
226 larger picture involving North Africa (Liu et al., 2001; Wu et al., 2009; He et al., 2017) and
227 portions of Eurasia via the so-called "silk road pattern" and "circumglobal teleconnection" (Lu et
228 al., 2002; Enomoto et al., 2003; Ding and Wang, 2005; Saeed et al., 2014; Wang et al., 2017;
229 Stephan et al., 2019, also see Chapter 13 and 14).

230 The monsoon-desert mechanism as first established using a linear modelling framework,
231 is also supported by relating prehistoric lake-levels to Milankovitch-monsoon forcing (Rodwell
232 and Hoskins, 1996) and extrapolated to the existence of "mega-deserts" and "mega-monsoon"
233 areas in specific periods (Wang et al., 2014). Evidences of moist events over east Sahara have

been observed (Gaven et al., 1981; Kowalski et al., 1989), consistent with shutting off of the monsoon-desert mechanism (Quade et al., 2018). Some of those wet events have been dated to correspond to minimum NH summertime insolation, linked with minimum intensity of ISM (Clemens et al., 1991). Some of these arguments have been confirmed with GCM studies (Claussen, 1994; Perez-Sanz et al., 2014).

As the ISM rainfall is projected to increase, the monsoon-desert teleconnection is consistent with the changes in 21st century projections over the Mediterranean region, at least for its central part corresponding to the largest increase in subsidence (Cherchi et al., 2016). However, other factors at play, i.e. like the warming and moistening of the troposphere under climate change, which enhance significantly the greenhouse effect over the deserts (Zhou, 2016; Wei et al., 2017), the North Atlantic Oscillation (Blade et al., 2012; Kalimeris and Kolios, 2019) or the changes in frequency/intensity of blocking systems (Masato et al., 2013; Tyrlis et al., 2015), may influence and shape the response in future climate projections. In future projections, the local atmospheric dynamics contribute in maintaining local temperature and precipitation balance over eastern and southern Mediterranean regions, suggesting a stronger influence of land surface warming on local atmospheric circulation and progressing desertification (Zhou, 2016; Wei et al., 2017; Barcikowska et al., 2020). In a climate change perspective, the influence from ISM on the Mediterranean region may have consequences also on the sea surface characteristics in terms of temperature and ecosystems (Kim et al., 2019).

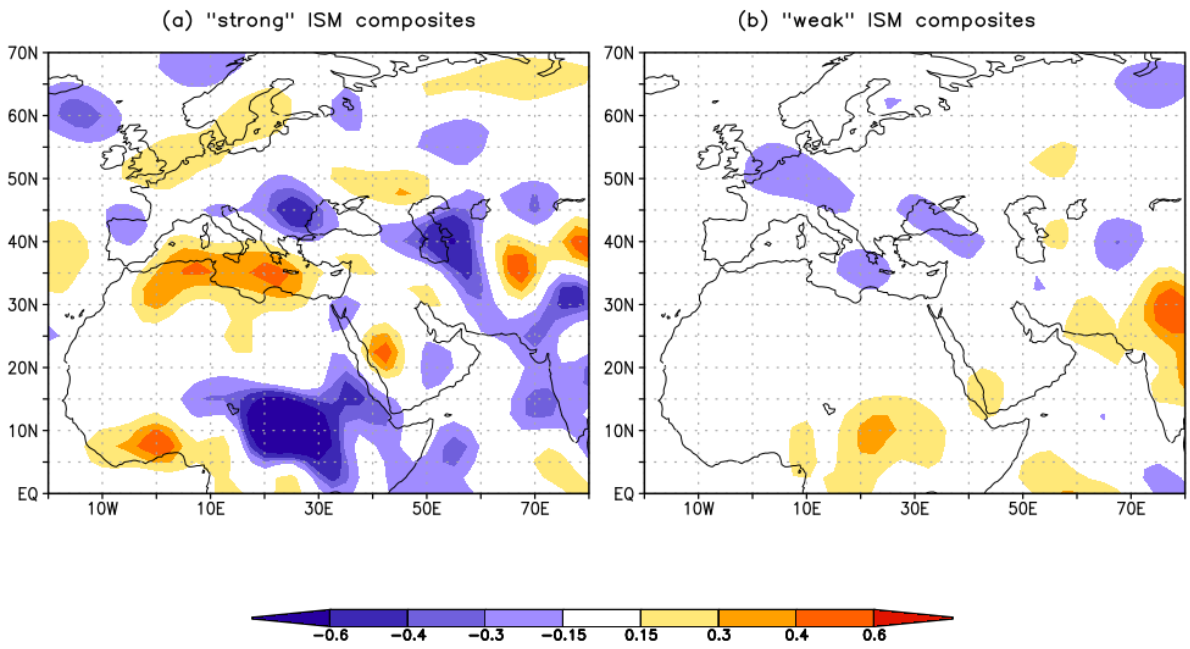

253

254 **Figure 15.4:** Composite of omega at 500 hPa (units hPa hr^{-1}) for (a) strong and (b) weak
255 monsoon years for the boreal summer monsoon period (June to September), using NCEP/NCAR
256 reanalysis dataset (Kalnay et al., 1996) for the period 1958-2019. Strong years are 1959, 1961,
257 1970, 1975, 1983, 1988, 1994 and weak years are 1965, 1966, 1968, 1972, 1974, 1979, 1982,
258 1985, 1986, 1987, 2002, 2004, 2009, 2014, 2015 (based on normalized All India Rainfall (AIR)
259 index exceeding 1 standard deviation). The AIR index is taken from
260 https://www.tropmet.res.in/~kolli/MOL/Monsoon/Historical/air.html.

261 **15.4 Potential role of deserts in modulating ISM**

262 The "monsoon-desert mechanism" described in the previous section, perceives the
263 subtropical deserts of the NH to be a rather "passive" recipient in the relationship. However,
264 from a different perspective, it is also argued that heat lows, changes of surface heating over the
265 subtropical deserts and dry air intrusions (whether natural or anthropogenic) from arid regions
266 into the monsoon domain can exert a significant control on the WAM and ISM systems, at both

267 the intra-seasonal and seasonal time scales (Charney, 1975; Charney et al., 1977; Shukla and
268 Mintz, 1982; Sud and Fennessy, 1982; Sud et al., 1988; Claussen, 1997; Bonfils et al., 2000;
269 Douville et al., 2001; Xue et al., 2004; Yasunari et al., 2006; Xue et al., 2010; Krishnamurti et
270 al., 2010; Bollasina and Nigam, 2011a, 2011b; Bollasina and Ming, 2013; Parker et al., 2016;
271 Terray et al., 2018; Sooraj et al., 2019). For example, Sahelian Heat Low plays a key-role in the
272 WAM evolution through its low-level cyclonic circulation and induced moisture convergence,
273 and this is well established in observations, reanalysis and GCM simulations (Haarsma et al.,
274 2005; Biasutti et al., 2009; Lavaysse et al., 2009; Shekhar and Boos, 2017). On similar lines,
275 ISM, especially its onset and early part, is known to be influenced by the atmospheric variability
276 over the subtropical desert regions (i.e., northwest part of India and west central Asia; Ramage,
277 1966; Smith, 1986a, 1986b; Mooley and Paolino 1988; Parthasarathy et al., 1992; Bollasina and
278 Nigam, 2011b; Bollasina and Ming, 2013; Vinoj et al., 2014; Rai et al., 2015; Sooraj et al.,
279 2019). During boreal summer, the monsoon depressions formed over the Bay of Bengal move
280 northwestward across the Indian landmass, and eventually merge and dissipate in the heat-low
281 region (Wang, 2006; Krishnamurti et al., 2013). The relationship between this seasonal heat low
282 and ISM has been examined in perpetual boreal spring atmospheric GCM (i.e., AGCM)
283 experiments by Bollasina and Ming, (2013). Remarkably, they found that the surface heating
284 (i.e., with no seasonal variation of insolation in their perpetual experiments) over northwestern
285 semi-arid areas is able to uniquely control the northwestward migration of ISM rainfall at
286 seasonal time scale and of the monsoon depressions at intra-seasonal time scale.

287 Furthermore, recent modeling studies show increasing evidence of the impact of dust
288 aerosols on the ISM at various time scales (i.e., from weekly to decadal) through aerosol
289 radiative effects (Ramanathan et al., 2005; Lau et al., 2006; Meehl et al., 2008; Wang et al.,

2009; Nigam and Bollasina, 2010; Bollasina et al., 2011; Vinoj et al., 2014; Jin et al., 2014, 2016a, 2016b; Solmon et al., 2015). For example, Vinoj et al. (2014) using AGCM sensitivity experiments argue that the presence of dust loading over North Africa and West Asian arid regions induced atmospheric heating over there, thus promoting abundant moisture transport into the ISM region, with associated enhanced rainfall (e.g., over Monsoon Core Region, MCZ). Thus, their study basically showed that the arid regions can also act as a dust induced atmospheric heat source (at least in a relative sense) during boreal summer and modulate ISM rainfall at the synoptic time scale. This is consistent with earlier studies (Smith 1986a, 1986b; Mohalfi et al., 1998), and also in line with other recent studies focusing on the impact of Middle East dust aerosols on ISM rainfall (Jin et al., 2014, 2015, 2016a; Solmon et al., 2015). However, the rainfall responses in each of these studies display heterogeneous distributions both in space and time (Solmon et al., 2015; Jin et al., 2016b; Sanap and Pandithurai, 2015). For example, Solmon et al. (2015) conducted a study (using a regional climate model) to examine the interaction between Middle East dust and ISM. Similar to Vinoj et al. (2014), they found an increase in rainfall restricted to the southern part of India with other parts, and central and northern India showing a significant decrease. Recently, Kumar and Arora, (2019) also claimed that enhanced dust forcing and associated warming over the Arabian Sea are unlikely to create a positive feedback on ISM rainfall, because of its limited spatial extent. To sum up, it is not altogether clear whether this part of the theory focusing on the role of Middle East dust on ISM is in definitive form.

This framework based on the relative heat source concept has also been extended to other time scales and to the ISM onset (Rai et al., 2015; Chakraborty and Agrawal, 2017; Samson et al., 2017; Terray et al., 2018; Sooraj et al., 2019). In particular, Samson et al. (2017) and Terray

et al. (2018) demonstrated the sensitivity of NH monsoon regions (in particular African-Asian monsoon) to the land surface thermal forcing over these arid regions. Using regional and global coupled GCMs, respectively, they modified the land surface albedo using up-to-date satellite estimates. According to them, the persistent tropical rainfall errors in current coupled GCMs are partly associated with insufficient surface thermal forcing and incorrect representation of the surface albedo over the NH continents. Improving the parameterization of the land albedo in a regional coupled model (Samson et al., 2017) and two global coupled GCMs (i.e., SINTEX; Masson et al., 2012 and CFSv2; Saha et al., 2014; Terray et al., 2018), leads to a significant reduction of the model systematic dry bias over land. They further showed that African-Asian monsoon circulation is, partly, a response to the large-scale pressure gradient between the hot NH subtropical deserts and the relatively cooler oceans to the south. A concept, which may have implications for the ISM response in the context of climate change as desertification has been identified as a robust feature of global warming (Zhou, 2016; Wei et al., 2017).

In a companion modeling study, Sooraj et al. (2019) found that ISM evolution and intensity are significantly affected with opposite polarity to prescribed negative and positive surface albedo perturbations over the whole hot subtropical desert lying to the west of ISM, including the remote Sahara Desert. This is consistent with the hypothesis that the arid regions can also act as a relative heat source and modulate the ISM, but also the whole tropical climate during boreal summer (Terray et al., 2018). The darkening of the deserts (negative albedo perturbations) leads to advancement of the ISM onset by one month, with a rapid northward propagation of the rainfall band over the Indian domain (see Fig. 15.5). The brightening of the deserts (i.e., positive albedo perturbation) shows non-linear response in ISM rainfall and circulation with significantly larger amplitude (figure not shown).

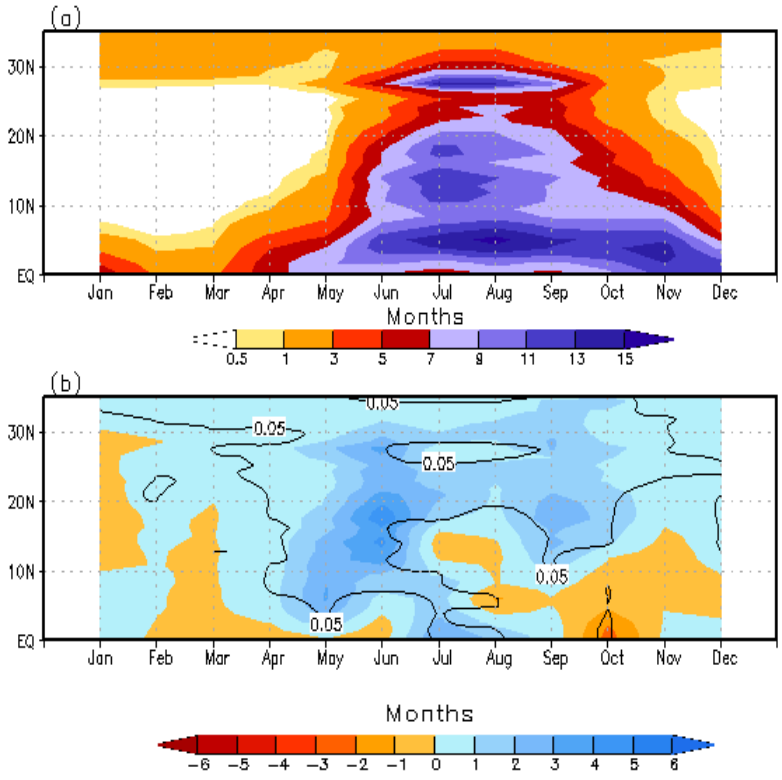

Figure 15.5: (a) Time-latitude evolution of rainfall climatology (mm day^{-1}) averaged along 70°-90°E (over both ocean and land points) from a control simulation performed with the SINTEX-F2 coupled model (Masson et al., 2012). (b) time-latitude evolution of anomalous rainfall response averaged along 70°-90°E from "Desert_m20" sensitivity experiment (see below). In (b), the responses that are above the 95% confidence level according to a permutation procedure with 9999 shuffles are encircled. "Desert_m20" is a sensitivity experiment performed with the SITEX-F2 coupled model in which the background land albedo has been artificially decreased by −20% over the whole hot subtropical desert extending up to the Sahara in the west (see highlighted box in Figure 15.1). [Adpated by permission from Sooraj et al., 2019]

Whilst the processes highlighted above (i.e., surface thermal forcing over arid regions) are mostly demonstrated at seasonal time scale, a recent observational study shows the evidence at the daily timescale as well (Sooraj et al., 2020). While examining the ISM rainfall extremes

over the MCZ region at daily time scale, these authors found that a similar surface thermal signature over Indo-Pakistan Arid Region (IPAR) is among the best precursors of the ISM wet daily extremes at longer lead times (e.g., one or two weeks in advance), outperforming Sea Surface Temperature precursors based on the Monsoon Intra-Seasonal Oscillation (e.g., Wang et al., 2005, Roxy et al., 2017). With the additional role of moist processes, the study revealed the surprising existence of a strong water vapour positive feedback over the drier IPAR, at intraseasonal and daily time scales, in line with the strong longwave greenhouse effect as found over arid regions in the context of global warming (Zhou, 2016; Wei et al., 2017). Further, according to their study, the enhanced surface warming and amplified water vapor feedbacks may be another significant contributor to the recent increasing trend in rainfall wet extremes over Indian landmass. In the backdrop of global warming, the results from Sooraj et al. (2020) may have larger implications concerning the changes in ISM rainfall extremes as well as their potential predictability.

15.5 Summary and future perspectives

This chapter presents a comprehensive review on the monsoon-desert system focusing on the mutual relationships between these two contrasting climates, which, surprisingly, coexist at the same latitude of the NH, and highlights the underlying mechanisms. Such a review assumes significance, as recently there is a renewed interest to understand the close relationships between the two systems since both of them are expected to be severely affected by anthropogenic climate change in the forthcoming decades.

Firstly, the literature focusing on the monsoon influence on subtropical deserts is reviewed by highlighting the monsoon-desert mechanism whereby convection over ISM (and also the neighboring Bay of Bengal) induces strong descending motions over the NH subtropical

373 deserts (i.e., to the west of ISM region), with the local subsidence and northerly flow (Etesian
374 winds) being manifestations of the Rossby wave structure associated with ISM convection (Fig.
375 15.3). These different processes are further summarized in Figure 15.6. Hence, the theoretical
376 framework, as suggested by earlier pioneering works (Rodwell and Hoskins, 1996, 2001), is now
377 well established from more recent observational and modeling studies (e.g., Uppala et al., 2005;
378 Tyrlis et al., 2013; Cherchi et al., 2014; Cherchi et al., 2018; Jin et al., 2019). Additional
379 evidences are also presented to show that the monsoon-desert mechanism and the underlying
380 processes operate at interannual timescales as well (Cherchi et al., 2014). However, most of the
381 state-of-the-art coupled GCMs are unable to simulate this monsoon-desert relationship, partly
382 due to the systematic monsoon dry bias affecting many current GCMs. For example, CMIP5
383 coupled GCMs with a severe dry bias over the ISM region depict the minimum descent over the
384 subtropical deserts (Cherchi et al., 2014). In future projections, the monsoon-desert relationship
385 remains elusive with ISM affecting mostly the central part of the Mediterranean region (Cherchi
386 et al., 2016), despite that desertification and ISM rainfall are both projected to increase during
387 the 21th century (Zhou, 2016; Wei et al., 2017; Wang et al., 2020). But, assessing the robustness
388 of this counter-intuitive signal is challenging for several reasons. For example, it is not known if
389 this paradox is related to the large uncertainty affecting ISM simulations (i.e., large biases in
390 ISM mean characteristics as mentioned above) in current coupled GCMs or if it is the sign of the
391 increasing role of radiative or surface land processes in shaping the climate of the deserts under
392 global warming. Furthermore, the subtropical deserts are also affected by large temperature and
393 radiation biases in current coupled GCMs (e.g., Samson et al., 2016; Terray et al., 2018). To sum
394 up, both significant modeling developments, and an exhaustive analysis of all the external

forcings at play (Blade et al., 2012; Kalimeris and Kolios, 2019; Masato et al., 2013; Tyrlis et al., 2015) are required to assess the fate of the monsoon-desert paradigm in our future world.

Secondly, we offered a different perspective by emphasizing the potential role of deserts in modulating ISM either through the changes of surface heating over the subtropical deserts or related to dry air intrusions from arid regions into the ISM domain (e.g., Krishnamurti et al., 2010; Bollasina and Nigam, 2011a, 2011b; Bollasina and Ming, 2013; Vinoj et al., 2014; Jin et al., 2014, 2016a; Solmon et al., 2015; Parker et al., 2016; Terray et al., 2018; Sooraj et al., 2019). Most of these studies, based on numerical modeling frameworks, show that the surface land warming paves the way for enhanced ISM rainfall through increased southwesterly monsoon flow and hence moist transport into the Indian continent. The associated processes are further summarized in Figure 15.6. For example, recent studies using fully coupled GCMs found that by darkening/brightening the subtropical deserts, the seasonality of ISM could be significantly modified (Fig. 15.5; e.g., Samson et al., 2017; Terray et al., 2018; Sooraj et al., 2019). Furthermore, a recent observational study provided new insights of the role of subtropical deserts (e.g., surface thermal forcing over IPAR) on the subseasonal modulations of ISM, and the occurrence of ISM daily rainfall extremes (Sooraj et al., 2020). These new studies challenge both the passive role of the desert as described in the monsoon-desert paradigm and the view that the lower tropospheric thermal contrast has only a minor role in the ISM evolution at different time scales from days to decades (Dai et al., 2013).

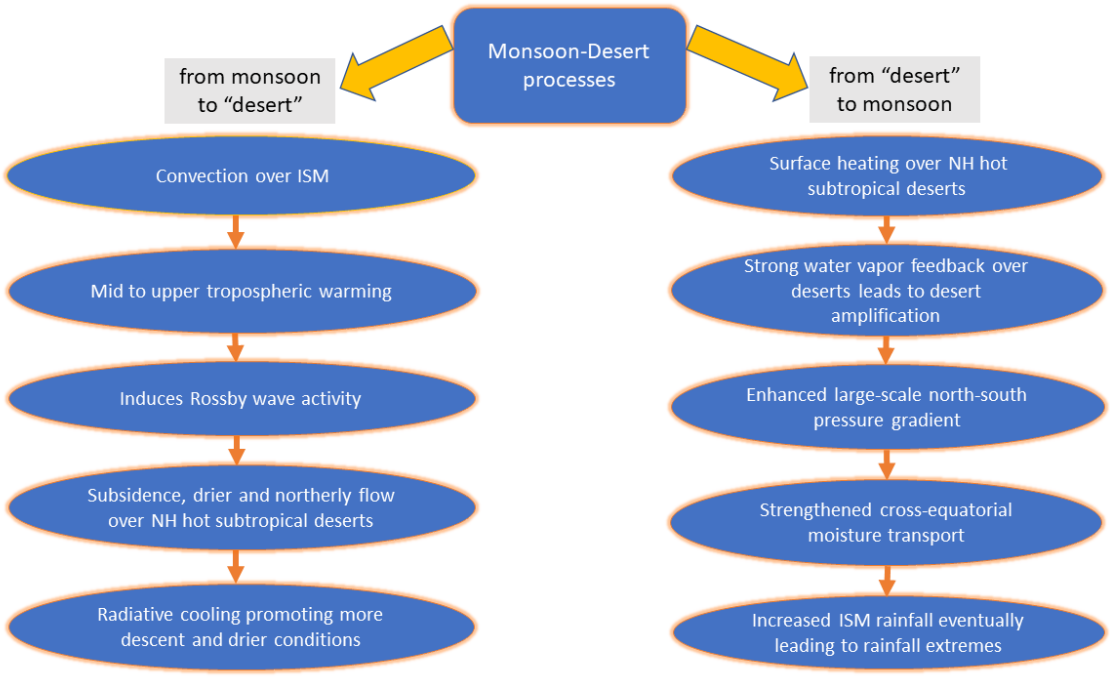

Figure 15.6: Schematic diagram summarizing the various interactive process and mechanisms in the monsoon-desert system over the African-Asian continent (i.e., from the monsoon to the "deserts" on the left and from the "deserts" to the monsoon on the right).

The subtropical deserts are particularly vulnerable to climate change (i.e., desert amplification with enhanced warming signal especially over the Sahara, the Arabian Peninsula and Middle-East) as suggested by several recent studies (e.g., Cook and Vizy, 2015; Zhou, 2016). The warming and moistening of the troposphere under climate change may in turn influence the local monsoon atmospheric circulation and, thus, eventually affect the monsoon-desert teleconnection in future climate. Further, the enhanced surface warming and amplified water vapor feedbacks over the arid regions adjacent to ISM (Sooraj et al., 2020) may have also significant implications for changes in frequency and intensity of ISM rainfall daily extremes under global warming scenario. However, as for the monsoon-desert mechanism, elucidating in a more robust way the potential role of the subtropical deserts on ISM will require both additional

428 analysis of observations and improved GCMs with reduced rainfall biases, more detailed
429 parameterizations for aerosols and improvements of the radiation codes embedded in these
430 models.

431

432

Conflict of interest statement

The corresponding author states no conflict of interest on behalf of all authors.

Acknowledgement

Pascal Terray is funded by Institut de Recherche pour le Développement (IRD, France). The Centre for Climate Change Research (CCCR) at Indian Institute of Tropical Meteorology (IITM) is fully funded by the Ministry of Earth Sciences, Government of India.

References

Annamalai, H., Taguchi, B., Sperber. K.R., McCreary, J.P., Ravichandran, M., Cherchi, A., Martin, G., Moise, A., 2015. Persistence of Systematic errors in the Asian-Australian monsoon Precipitation in climate models: a way forward. Clivar. Exchanges. 66 doi:10.2172/1178403

Attada, R., Dasari, H.P., Parekh, A., Chowdary, J.S., Langodan, S., Knio, O., Hoteit, I., 2019. The role of the Indian summer monsoon variability on Arabian Peninsula summer climate. Clim. Dyn. 52, 3389-3404 doi: 10.1007/s00382-018-4333-x

Barcikowska, M.J., Kapnick, S.B., Krishnamurty, L., Russo, S., Cherchi, A., Folland, C.K., 2020. Changes in the future summer Mediterranean climate: contribution of teleconnections and local factors. Earth. Syst. Dyn. 11, 161-181 doi: 10.5194/esd-11-161-2020

Biasutti, M., Sobel, A.H., Camargo, S.J., 2009. The role of the Sahara low in summertime Sahel rainfall variability and change in the CMIP3 models. J. Clim. 22, 5755–5771. doi:10.1175/2009JCLI2969.1

Blade, I., Liebmann, B., Fortuny, D., van Oldenborgh, G.J., 2012. Observed and simulated impacts of the summer NAO in Europe: implications for projected drying in the Mediterranean region. Clim. Dyn. 39, 709-727 doi: 10.1007/s00382-011-1195-x

Bollasina, M., Ming, Y., 2013. The role of land-surface processes in modulating the Indian monsoon annual cycle. Clim. Dyn. 41(9–10),2497–2509. doi:10.1007/s00382-012-1634-3

Bollasina, M., Nigam, S., 2011a. The summertime “heat” low over Pakistan/northwestern India: evolution and origin. Clim. Dyn. 37, 957–970

462 Bollasina, M., Nigam, S., 2011b. Modeling of regional hydroclimate change over the Indian
463 subcontinent: impact of the expanding Thar desert. J. Clim. 24, 3089–3106

464 Bollasina, M.A., Ming, Y., Ramaswamy, V., 2011. Anthropogenic aerosols and the weakening
465 of the South Asian summer monsoon. Science. 334, 502–505, doi:10.1126/science.1204994

466 Bonfils, C., Noblet-Ducoudré, N.de., Braconnot, P., Joussaume, S., 2000. Hot desert albedo and
467 climate change: Mid-Holocene monsoon in North Africa. J. Clim. 14, 3724–3737.

468 Chakraborty, A., Agrawal, S., 2017. Role of west Asian surface pressure in summer monsoon
469 onset over central India. Environ. Res. Lett. 12

470 Charney, J.G., 1975. Dynamics of deserts and drought in Sahel. Quart. J. Roy. Meteor. Soc. 101:
471 193-202.

472 Charney, J., Quirk, W.J., Chow. S., Kornfield, J., 1977. A comparative study of the effects of
473 albedo change on drought in semi-arid regions. J. Atmos. Sci. 34, 1366–1385.

474 Cherchi, A., Annamalai, H., Masina, S., Navarra, A.,2014. South Asian summer monsoon and
475 the eastern Mediterranean climate: the monsoon-desert mechanism in CMIP5 simulations. J.
476 Clim. 27, 6877-6903 doi: 10.1175/JCLI-D-13-00530.1

477 Cherchi, A., Annamalai, H., Masina, S., Navarra, A., Alessandri, A., 2016. Twenty-first century
478 projected summer mean climate in the Mediterranean interpreted through the monsoon-desert
479 mechanism. Clim. Dyn. 47, 2361-2371 doi: 101007/s00382-015-2968-4

480 Cherchi, A., Ambrizzi, T., Behera, S., Freitas, A.C.V., Morioka, Y., Zhou, T., 2018. The
481 response of subtropical highs to climate change. Curr. Clim. Ch. Rep. doi: 10.1007/s40641-018-
482 0114-1

Claussen, M., 1994. On coupling global biome models with climate models. Clim. Res. 4, 203-221

Claussen, M., 1997. Modeling biogeophysical feedback in the Africa and India monsoon region. Clim. Dyn. 13:247–257.

Clemens, S., Prell, W., Murray, D., Shimmield, G., Weedon, G., 1991. Forcing mechanisms of the Indian Ocean monsoon. Nature. 353, 720-725 doi: 10.1038/353720a0

Cook, K.H., Vizy, E.K., 2015. Detection and analysis of an amplified warming of the Sahara Desert. J. Clim. 28, 6560–6580, doi:10.1175/JCLI-D-14-00230.1

Dai, A., Li, H., Sun, Y., Hong, L.-C., Ho, Lin., Chou, C., and Zhou, T., 2013. The relative roles of upper and lower tropospheric thermal contrasts and tropical influences in driving Asian summer monsoons, J. Geophys. Res. Atmos. 118, 7024–7045, doi:10.1002/jgrd.50565.

Dee, D.P., Uppala, S.M., Simmons, A.J., Berrisford, P., Poli, P., Kobayashi, S., Andrae, U., Balmaseda, M.A., Balsamo, G., Bauer, P., Bechtold, P., Beljaars, A.C.M., van de Berg, L., Bidlot, J., Bormann, N., Delsol, C., Dragani, R., Fuentes, M., Geer, A.J., Haimberger, L., Healy, S.B., Hersbach, H., Hólm, E.V., Isaksen, L., Kållberg, P., Köhler, M., Matricardi, M., McNally, A.P., Monge-Sanz, B.M., Morcrette, J.-J., Park, B.-K., Peubey, C., de Rosnay, P., Tavolato, C., Thépaut, J.-N. and Vitart, F., 2011. The ERA-Interim reanalysis: Configuration 683 and performance of the data assimilation system. Quart. J. Roy. Meteorol. Soc. 137:553–597.

Ding, Q.H., Wang, B., 2005. Circumglobal teleconnection in the Northern Hemisphere summer. J. Clim. 18, 3483-3505 doi: 10.1175/JCLI3473.

503 Douville, H., Chauvin, F., Broqua, H., 2001. Influence of soil moisture on the Asian and African
504 monsoons. Part I: Mean monsoon and daily precipitation. J. Clim. 14, 2381–2403

505 Enomoto, T., Hoskins, B. J., Matsuda,Y., 2003. The formation mechanism of the Bonin high in
506 August. Quart. J. Roy. Meteor. Soc. 129, 157-178 doi: 10.1256/qj.01.211

507 Gaven, C., Hillaire-Marcel, C., Petit-Marie, N., 1981. A Pleistocene lacustrine episode in south-
508 eastern Libya. Nature. 290, 131-133 doi: 10.1038/290131a0

509 Haarsma, R. J., Selten, F. M., Weber, S. L., Kliphuis, M., 2005. Sahel rainfall variability and
510 response to greenhouse warming. Geophys. Res. Lett. 32, L17702

511 He, S., Yang, S., Li, Z., 2017. Influence of latent heating over the Asian and Western Pacific
512 monsoon region on Sahel summer rainfall. Sci. Rep. 7, 7680 doi: 10.1038/s41598-017-07971-6

513 Haywood, J. M.,Jones, A., Dunstone, N., Milton, S., Vellinga, M., Bodas□Salcedo, A.,
514 Hawcroft, M., Kravitz, B., Cole, J., Watanabe, S., Stephens, G., 2016. The impact of
515 equilibrating hemispheric albedos on tropical performance in the HadGEM2-ES coupled climate
516 model, Geophys. Res. Lett. 43, 395–403, doi:10.1002/2015GL066903.

517 Hoskins, B. J., 1986. Diagnosis of forced and free variability in the atmosphere, pp. 57–63, in:
518 Atmospheric and Oceanic Variability, edited by: Cattle, H., Royal Meteorological Society,
519 Bracknell.

520 Huffman, G. J., Adler, R. F., Bolvin, D. T., Gu, G., 2009. Improving the global precipitation
521 record: GPCP Version 2.1. Geophy. Res. Lett. 36,L17808. doi:10.1029/2009GL040000

522 IPCC, 2013. Fifth Assessment Report of the Intergovernmental Panel on Climate Change,
523 www.ipcc.ch/ipccreports/ar4-wg1.htm

524 Jin, L., Zhang, H., Moise, A., Martin, G., Milton, S., Rodriguez, J., 2019. Australia-Asian
525 monsoon in two versions of the UK Met Office Unified Model and their impacts on tropical-
526 extratropical teleconnections. Clim. Dyn. 53, 4717-4741 doi: 10.1007/s00382-019-04821-1

527 Jin, Q., Wei, J., Yang, Z.L., 2014. Positive response of Indian summer rainfall to Middle East
528 dust. Geophys. Res. Lett. 41,4068–4074. https://doi.org/10.1002/2014GL059980

529 Jin, Q., Wei, J., Yang, Z.L., Pu, B., Huang, J., 2015. Consistent response of Indian summer
530 monsoon to Middle East dust in observations and simulations. Atmos. Chem. Phys. 15,9897–
531 9915. https://doi.org/10.5194/acp-15-9897-2015

532 Jin, Q., Yang, Z.-L., Wei, J., 2016a. High sensitivity of Indian summer monsoon to Middle East
533 dust absorptive properties. Sci. Rep. 6, 30690, doi:10.1038/srep30690.

534 Jin, Q., Yang, Z.-L., Wei, J., 2016b. Seasonal responses of Indian summer monsoon to dust
535 aerosols in the Middle East, India, and China. J. Clim. 29, 6329–6349

536 Kalimeris, A., Kolios, S., 2019. TRMM-based rainfall variability over the central Mediterranean
537 and its relationship with atmospheric and oceanic climatic modes. Atm. Res. 230, 104649 doi:
538 10.1016/j.atmosres.2019.104649

539 Kalnay, E., Kanamitsu, M., Kirtler, R., Collins, W., Deaven, D., Gandin, L., Iredell, M., Saha, S.,
540 White, G., Woollen, J., Zhu, Y., Chelliah, M., Ebisuzaki, W., Higgins, W., Janowiak, J., Mo, K.
541 C., Ropelewski, C., Wang, J., Leetma, A., Reynolds, R., Jenne, R., Joseph, D., 1996. The
542 NCEP/NCAR 40-year reanalysis project. Bull. Amer. Meteor. Soc. 77, 437-470

543 Kato, S., Rose, F. G., Rutan, D. A., Thorsen, T. J., Loeb, N. G., Doelling, D. R., et al 2018.
544 Surface irradiances of Edition 4.0 Clouds and the Earth's Radiant Energy System (CERES)

545 Energy Balanced and Filled (EBAF) data product. J. Clim. 31, 4501–4527. doi: 10.1175/JCLI-D-
546 17-0523.1

547 Kim, G-U., Seo K-H., Chen, D., 2019. Climate change over the Mediterranean and current
548 destruction of marine ecosystem. Sci. Rep. 9, 18813 doi: 10.1038/s41598-019-55303-7

549 Kitoh, A., 2017. The Asian monsoon and its future change in climate models: a review. J.
550 Meteor. Soc. Japan. 95, 7-33, doi:10.2151/jmsj.2017-002.

551 Kowalski, K., Van Neer, W., Bochenski, Z., Mlynarski, M., Rsebik-Kowalska, B., Szyndlar, Z.,
552 Lavaysse, C., Flamant, C., Janicot, S., Parker, D.J., Lafore, J.P., Sultan, B., Pelon, J., 2009.
553 Seasonal evolution of the West African heat low: a climatological perspective. Clim. Dyn. 33,
554 313–330

555 Krishnamurti, T.N., Thomas, A., Simon, A., Kumar, V., 2010. Desert air incursions, an
556 overlooked aspect, for the dry spells of the Indian summer monsoon. J. Atmos. Sci. 67, 3423–
557 3441

558 Krishnamurti, T.N., Stefanova, L., Misra, V., 2013. Tropical meteorology (pp 331). Springer.
559 New York, NY.

560 Krishnan, R., Sabin, T.P., Vellore, R., Mujumdar, M., Sanjay, J., Goswami, B.N., Hourdin, F.,
561 Dufresne J-L., Terray, P., 2016. Deciphering the desiccation trend of the South Asian monsoon
562 hydroclimate in a warming world. Clim. Dyn. 47(3–4),1007–1027.
563 https://doi.org/10.1007/s00382-015-2886-5

564 Kumar, S., Arora, A., 2019. On the connection between remote dust aerosol and Indian summer
565 monsoon. Theor. Appl. Climatol. 137, 929–940. https://doi.org/10.1007/s00704-018-2647-6

566 Lau, K. M., Kim, M. K., Kim, K. M., 2006. Asian summer monsoon anomalies induced by
567 aerosol direct forcing: The role of the Tibetan Plateau. Clim. Dyn. 26, 855–864,
568 doi:10.1007/s00382-006-0114-z.

569 Lavaysse, C., Flamant, C., Janicot, S., Parker, D.J., Lafore, J.P., Sultan, B., Pelon, J., 2009.
570 Seasonal evolution of the West African heat low: a climatological perspective. Clim. Dyn. 33:
571 313–330

572 Levine, R.C., Turner, A.G., Marathayil, D., Martin, G.M., 2013. The role of northern Arabian
573 Sea surface temperature biases in CMIP5 model simulations and future predictions of Indian
574 summer monsoon rainfall. Clim. Dyn. 41: 155–172

575 Liu, P., Wu, G., Sun, S., 2001. Local meridional circulation and deserts. Adv. Atmos. Sci. 18,
576 864-872 doi: 10.1007/BF03403508

577 Lu, R.Y., Oh, J.H., Kim, B. J., 2002. A teleconnection pattern in upper-level meridional wind
578 over the North African and Eurasian continent in summer. Tellus. 54A: 44-55 doi:
579 10.3402/tellusa.v54i1.12122

580 Masato, G., Hoskins, B. J., Woollings, T., 2013. Winter and summer northern hemisphere
581 blocking in CMIP5 models. J. Clim. 26, 7044-7059 doi: 10.1175/JCLI-D-12-00466.1

582 Masson, S., Terray, P., Madec, G., Luo, J. J., Yamagata, T., Takahashi, K., 2012. Impact of intra-
583 daily SST variability on ENSO characteristics in a coupled model. Clim. Dyn. 39,681-707

584 Meehl, G. A., Arblaster, J. M., Collins, W. D., 2008. Effects of black carbon aerosols on the
585 Indian monsoon. J. Clim. 21, 2869–2882, doi:10.1175/2007JCLI1777.1

586 Mohalfi, S., Bedi, H.S., Krishnamurti, T.N., Cocke, S.D., 1998. Impact of shortwave radiative
587 effects of dust aerosols on the summer season heat low over Saudi Arabia. Mon. Wea. Rev. 126,
588 3153–3168

589 Mooley, D.A., Paolino, D.A., 1988. A predictive monsoon signal in the surface level thermal
590 fields over India. Mon. Wea. Rev. 116,256–264

591 Neelin, J.D., Held, I.M., 1987. Modeling tropical convergence based on the moist static energy
592 budget. Mon. Wea. Rev. 115:3–12

593 Nigam, S., Bollasina, M., 2010. ‘‘Elevated heat pump’’ hypothesis for the aerosol-monsoon
594 hydroclimate link: ‘‘Grounded’’ in observations? J. Geophys. Res. 115, D16201,
595 doi:10.1029/2009JD013800.

596 Osso, A., Shaffrey, L., Dong, B., Sutton, R., 2019. Impact of air-sea coupling on Northern
597 Hemisphere summer climate and the monsoon-desert teleconnection. Clim. Dyn. 53, 5063-5078
598 doi: 10.1007/s00382-019-04846-6

599 Parker, D.J., Willetts, P., Birch, C., Turner, A.G., Marsham, J. H., Taylor, C.M., Kolusu, S.,
600 Martin, G. M., 2016. The interaction of moist convection and mid-level dry air in the advance of
601 the onset of the Indian monsoon. Quart. J. Roy. Meteor. Soc. 142, 2256–2272,
602 https://doi.org/10.1002/qj.2815.

603 Parthasarathy, B., Rupakumar, K., Munot, A.A., 1992 . Surface pressure and summer monsoon
604 rainfall over India. Adv. Atmos. Sci. 9,359–366

Perez-Sanz, A., Li, G., Gonzalez-Samperiz, P., Harrison, S. P., 2014. Evaluation of modern and mid-Holocene seasonal precipitation of the Mediterranean and northern Africa in the CMIP5 simulations. Clim. Past. 10, 551-568 doi: 10.5194/cp-10-551-2014

Prodhomme, C., Terray, P., Masson, S., Izumo, T., Tozuka, T., Tamagata, T., 2014. Impacts of Indian Ocean SST biases on the Indian Monsoon as simulated in a global coupled model. Clim. Dyn. 42:271–290

Quade, J., Dente, E., Armon, M., Ben Dor, Y., Morin, E., Adam, O., Enzel, Y., 2018. Megalakes in the Sahara? A review. Quart. Res. 90, 235-275 doi: 10.1017/qua.2018.46

Rai, A., Saha, S.K., Pokhrel, S., Sujith, K., Halder, S., 2015. Influence of pre-onset land-atmospheric conditions on the Indian summer monsoon rainfall variability. J. Geophys. Res. Atmos. 120:4551–4563

Ramage, C.S., 1966. The summer atmospheric circulation over the Arabian Sea. J. Atmos. Sci. 23, 144–150.

Ramanathan, V., Chung, C., Kim, D., Bettge, T., Buja, L., Kiehl, J. T.,Washington, W. M, Fu, Q., Sikka, D. R., Wild, M., 2005. Atmospheric brown clouds: Impacts on South Asian climate and hydrological cycle. Proc. Natl. Acad. Sci. USA, 102, 5326–5333, doi:10.1073/pnas.0500656102.

Rizou, D., Flocas, H.A., Hatzaki, M., Bartzokas, A., 2018. A statistical investigation of the impact of the Indian monsoon on the eastern Mediterranean circulation. Atmosphere. 9 doi: 10.3390/atmos9030090

625 Rodwell, M.J., Hoskins, B.J., 1996. Monsoons and the dynamics of deserts. Quart. J. Roy.
626 Meteor. Soc. 122, 1385-1404

627 Rodwell, M.J., Hoskins, B.J., 2001. Subtropical anticyclones and summer monsoons. J. Clim. 14,
628 3192-3211

629 Roehrig, R., Bouniol, D., Guichard, F., Hourdin, F., Redelsperger, J.L., 2013 The present and
630 future of the West African monsoon: a process-oriented assessment of CMIP5 simulations along
631 the AMMA Transect. J. Clim. 26: 6471–6505

632 Roxy, M.K., Ghosh, S., Pathak, A., Athulya, R., Mujumdar, M., Murtugudde, R., Terray, P.,
633 Rajeevan, M., 2017. A threefold rise in widespread extreme rain events over central India. Nat.
634 Commun. 1-11. doi:10.1038/s41467-017-00744-9

635 Sabeerali, C.T., Rao, S.A., Dhakate, A.R., Salunke, K., Goswami, B.N., 2015. Why ensemble
636 mean projection of south Asian monsoon rainfall by CMIP5 models is not reliable? Clim. Dyn.
637 45, 161–174

638 Saeed, S., Lipzig, N.V., Muller, W.A., Saeed, F., Zanchettin, D., 2014. Influence of the
639 circumglobal wave train on European summer precipitation. Clim. Dyn. 43, 503-515 doi:
640 10.1007/s00382-013-1871-0

641 Saha, S., Moorthi, S.,Wu, X.,Wang, J., Pan, H.-L.,Wang, J., Nadiga, S., Tripp, P., Behringer, D.,
642 Hou, Y.T., Chuang, H.Y., Iredell, M., Ek, M., Meng, J., Yang, R., Mensez, M.P., Dool, H.V.D.,
643 Zhang, Q., Wang, W., Chen, M. and Becker, E., 2014. The NCEP climate forecast system
644 version 2. J. Clim. 27,2185–2208

645 Samson, G., Masson, S., Durand, F., Terray, P., Berthet, S., Jullien, S., 2017. Role of land
646 surface albedo and horizontal resolution on the Indian Summer Monsoon biases in a coupled
647 ocean-atmosphere tropical-channel model. Clim. Dyn. doi:10.1007/s00382-016-3161-0

648 Sanap, S.D., Pandithurai, G., 2015. Inter-annual variability of aerosols and its relationship with
649 regional climate over Indian subcontinent. Int. J. Climatol. 35,1041–1053.
650 https://doi.org/10.1002/joc.4037

651 Sandeep, S., Ajayamohan, R., 2015. Origin of cold bias over the Arabian Sea in Climate Models.
652 Sci. Rep. 4, 6403. https://doi.org/10.1038/srep06403

653 Shekhar, R., Boos, W.R., 2017. Weakening and Shifting of the Saharan Heat Low Circulation
654 During Wet Years of the West African Monsoon. J. Clim. 30, 7399-7422

655 Shukla, J., Mintz, Y., 1982. Influence of land-surface evaporation on Earth's climate. Science.
656 215, 1498–1501

657 Sikka, D.R., 1997. Desert climate and its dynamics. Curr. Sci. 72, 35–46.

658 Singh, R., AchutaRao, K., 2018. Quantifying uncertainty in twenty-first century climate change
659 over India. Clim. Dyn. 52(7–8), 3905–3928. https://doi.org/10.1007/s00382-018-4361-6

660 Smith, E.A., 1986a. The structure of the Arabian heat low. Part I: surface energy budget. Mon.
661 Wea. Rev. 114, 1067–1083.

662 Smith, E.A., 1986b. The structure of the Arabian heat low. Part II: bulk tropospheric heat budget
663 and implications. Mon. Wea. Rev. 114, 1084–1102

664 Solmon, F., Nair, V.S., Mallet, M., 2015. Increasing Arabian dust activity and the Indian summer
665 monsoon. Atmos. Chem. Phys. 15, 8051–8064. https://doi.org/10.5194/acp-15-8051-2015

666 Sooraj, K.P., Terray, P., Mujumdar, M., 2015. Global warming and the weakening of the Asian
667 summer monsoon circulation: assessments from the CMIP5 models. Clim. Dyn. 45, 233–252.

668 Sooraj, K.P., Terray, P., Masson, S., Cretat, J., 2019. Modulations of the Indian summer
669 monsoon by the hot subtropical deserts: insights from coupled sensitivity experiments. Clim.
670 Dyn. 52, 4527–4555. https://doi.org/10.1007/s00382-018-4396-8.

671 Sooraj, K.P., Terray, P., Shilin, A., Mujumdar, M., 2020. Dynamics of rainfall extremes over
672 India: A new perspective. Int. J. Climatol. 40: 5223– 5245. https://doi.org/10.1002/joc.6516

673 Sperber, K.R., Annamalai, H., Kang, I.S., Kitoh, A., Moise, A., Turner, A.G., Wang, B., Zhou,
674 T., 2013. The Asian summer monsoon: an intercomparison of CMIP5 vs. CMIP3 simulations of
675 the late 20th century. Clim. Dyn. 41: 2711–2744. doi:10.1007/s00382-012-1607-6

676 Stephan, C.C., Klingaman, N.P., Turner, A.G., 2019. A mechanism for the recently increased
677 interdecadal variability of the Silk Road Pattern. J. Clim. 32, 717-736 doi: 10.1175/JCLI-D-18-
678 0405.1

679 Sud, Y.C., Fennessy, M., 1982. A study of the influence of surface albedo on July circulation in
680 semi-arid regions using the GLAS GCM. Int. J. Climatol. 2, 105–125.

681 Sud, Y.C., Shukla, J., Mintz, Y., 1988. Influence of land surface roughness on atmospheric
682 circulation and precipitation: A sensitivity study with a general circulation model. J. Appl.
683 Meteor. 27, 1036–1054.

684 Taylor, K., Stouffer, R., Meehl, G., 2012. An overview of CMIP5 and the experiment design.
685 Bull. Am. Meteor. Soc. 93, 485-498 doi: 10.1175/BAMS-D-11-00094.1

686 Terray, P., Sooraj, K.P., Masson, S., Krishna, R.P.M., Samson, G., Prajeesh, A.G., 2018.
687 Towards a realistic simulation of boreal summer tropical rainfall climatology in state-of the-art
688 climate coupled models. Clim. Dyn. 50, 3413–3439 doi:10.1007/s00382-017-3812-9

689 Tyrlis, E., Lelieveld, J., Steil, B., 2013. The summer circulation over the eastern Mediterranean
690 and the Middle East: influence of the South Asian monsoon. Clim. Dyn. 40, 1103-1123 doi:
691 10.1007/s00382-012-1528-4

692 Tyrlis, E., Tymvios, F.S., Giannakopoulos, C., Lelieveld, J., 2015. The role of blocking in the
693 summer 2014 collapse of Etesians over the eastern Mediterranean. J. Geophys. Res. Atm. 120,
694 6777-6792 doi: 10.1002/2015JD023543

695 Uppala, S.M., Kallberg, P.W., Simmons, A.J., et al 2005. The ERA-40 Reanalysis. Quart. J. Roy.
696 Meteor. Soc. 131, 2961-3012 doi: 10.1256/qj.04.176

697 Vinoj, V., Rasch, P. J., Wang, H., Yoon, J. H., Ma, P. L., Landu, K., Singh, B., 2014. Short term
698 modulation of Indian summer monsoon rainfall by West Asian dust. Nature. Geo. Science.
699 doi:10.1038/NGEO2017

700 Wang, B., 2006. The Asian Monsoon. Springer, Chichester.

701 Wang, B., Biasutti, M., Byrne, M., Castro, C., Chang, C. P., et al., 2020. Monsoons Climate
702 Change Assessment. Bull. Amer. Meteor. Soc. doi: https://doi.org/10.1175/BAMS-D-19-0335.1.

703 Wang, B., Liu, J., Kim, H.J., Webster, P.J., Yim, S.Y., 2012. Recent change of the global
704 monsoon precipitation (1979-2008). Clim. Dyn. 39, 1123-1135 doi: 10.1007/s00382-011-1266-z

705 Wang, B., Webster, P.J., Teng, H., 2005. Antecedents and self-induction of active-break south
706 Asian monsoon unraveled by satellites. Geophys. Res. Lett. 32, 4–7
707 doi:10.1029/2004GL020996

708 Wang, C., Kim, D., Ekman, A. M. L., Barth, M. C., Rasch, P. J., 2009. Impact of anthropogenic
709 aerosols on Indian summer monsoon. Geophys. Res. Lett. 36, L21704
710 doi:10.1029/2009GL040114.

711 Wang, L., Xu, P., Chen, W., Liu, Y., 2017. Interdecadal variations of the Silk Road Pattern. J.
712 Clim. 30, 9915-9932 doi: 10.1175/JCLI-D-17-0340.1

713 Wang, P.X., Wang, B., Cheng, H., Fasullo, J., Guo, Z.T., Kiefer, T., Liu, Z.Y., 2014. The global
714 monsoon across timescales: coherent variability of regional monsoons. Clim. Past. 10, 2007-
715 2052 doi: 10.5194/cp-10-2007-2014

716 Warner, T.T., 2004. Desert Meteorology Cambridge University Press, London, p 612

717 Webster, P.J., 1994. The role of hydrological processes in ocean atmosphere interactions. Rev.
718 Geophys. 32(4), 427–476

719 Wei, N., Zhou, L., Dai, Y., Xia, G., Hua, W., 2017. Observational Evidence for Desert
720 Amplification Using Multiple Satellite Datasets. Sci. Rep. 2043 doi:10.1038/s41598-017-02064-
721 w

722 Wu, G.X., Liu, Y., Zhu, X., Li, W., Ren, R., Duan, A., Liang, X., 2009. Multi-scale forcing and
723 the formation of subtropical desert and monsoon. Ann. Geophys. 27, 3631-3644 doi:
724 10.5194/angeo-27-3631-2009

725 Xue, Y., Juang, H.M.H., Li, W. P., Prince, S., Defries, R., Jiao, Y., Vasic, R., 2004. Role of land
726 surface processes in monsoon development: East Asia and West Africa. J. Geophys. Res.
727 (Atmos). 109, 03105–03128

728 Xue, Y., De, Sales F., Vasic, R., Mechoso, C. R., Prince, S. D., Arakawa, A., 2010. Global and
729 temporal characteristics of seasonal climate/vegetation biophysical process (VBP) interactions. J.
730 Clim. 23, 1411–1433

731 Yang, S., Webster, P.J., Dong, M., 1992. Longitudinal heating gradient: another possible factor
732 influencing the intensity of the Asian summer monsoon circulation. Adv. Atmos. Sci. 9, 397-410

733 Yasunari, T., Saito, K., Takata, K., 2006. Relative roles of large-scale orography and land
734 surface processes in the global hydroclimate, Part I: Impacts on monsoon systems and the
735 Tropics. J. Hydrometeor. 7: 626–641.

736 Zhou, L., 2016. Desert amplification in a warming climate. Sci. Rep. 6. doi:10.1038/srep31065

737

738 **Figure captions:**

739 **Figure 15.1**: Climatological map of (a) rainfall (mm day^{-1}), (b) land surface albedo (%) and (c)
740 net radiation budget at TOA (Wm^{-2}), for boreal summer period (June to September). In (a)
741 rainfall climatology is computed for the 1986-2014 period from Global Precipitation
742 Climatology Project (GPCP version 2.1; Huffman et al., 2009). In (b) and (c), albedo and
743 radiation climatology is computed for the 2000-2018 period from the Clouds and the Earth's
744 Radiant Energy System Energy Balanced and Filled (CERES-EBAF edition 4.0; Kato et al.,
745 2018). In (b) and (c), the region highlighted in the black rectangle refers to "subtropical deserts".

746 **Figure 15.2:** Vertical cross-section of atmospheric circulation in terms of vertical component of
747 velocity (10^{-2} Pa s^{-1}, shaded) and horizontal wind divergence (10^{-6} s^{-1}, contours) during July,
748 along a pressure-longitude plane averaged over two latitude bands (a) 20°N and (b) 40°N. The
749 circulation fields are taken from the ERA-Interim reanalysis (Dee et al., 2011) and the
750 climatology is computed for the 1986-2014 period. The negative (dashed) and positive
751 (continuous) contours correspond, respectively, to absolute magnitudes of 1, 2, 3 and 4 units.
752 The zero contours are highlighted in thick black color. Negative (positive) shading implies
753 ascending (descending), while negative (positive) contours implies convergence (divergence).
754 The presentation using July climatology follows the observational conjecture that it corresponds
755 to the peak of monsoon activity (e.g., Tyrlis et al., 2013).

756 **Figure 15.3:** (a) Schematic diagram of the monsoon desert-mechanism with descent over the
757 desert region (orange) induced by the heating over the monsoon convective region (cyan)
758 interacting with local westerlies. [Adapted by permission from Wang et al., 2012]. (b) JJA mean
759 wind (ms^{-1}, green vectors), meridional wind velocity (ms^{-1}, shaded), and pressure levels (hPa,

760 contours with 50-hPa contour interval) on isentropic surfaces at 325K using NCEP/NCAR
761 reanalysis dataset (Kalnay et al., 1996). The climatology is computed for the period 1958-2019.
762 **Figure 15.4:** Composite of omega at 500 hPa (units hPa hr^{-1}) for (a) strong and (b) weak
763 monsoon years for the boreal summer monsoon period (June to September), using NCEP/NCAR
764 reanalysis dataset (Kalnay et al., 1996) for the period 1958-2019. Strong years are 1959, 1961,
765 1970, 1975, 1983, 1988, 1994 and weak years are 1965, 1966, 1968, 1972, 1974, 1979, 1982,
766 1985, 1986, 1987, 2002, 2004, 2009, 2014, 2015 (based on normalized All India Rainfall (AIR)
767 index exceeding 1 standard deviation). The AIR index is taken from
768 https://www.tropmet.res.in/~kolli/MOL/Monsoon/Historical/air.html.
769 **Figure 15.5:** (a) Time-latitude evolution of rainfall climatology (mm day^{-1}) averaged along 70°-
770 90°E (over both ocean and land points) from a control simulation performed with the SINTEX-
771 F2 coupled model (Masson et al., 2012). (b) time-latitude evolution of anomalous rainfall
772 response averaged along 70°-90°E from "Desert_m20" sensitivity experiment (see below). In
773 (b), the responses that are above the 95% confidence level according to a permutation procedure
774 with 9999 shuffles are encircled. "Desert_m20" is a sensitivity experiment performed with the
775 SITEX-F2 coupled model in which the background land albedo has been artificially decreased
776 by −20% over the whole hot subtropical desert extending up to the Sahara in the west (see
777 highlighted box in Figure 15.1). [Adpated by permission from Sooraj et al., 2019]
778 **Figure 15.6:** Schematic diagram summarizing the various interactive process and mechanisms in
779 the monsoon-desert system over the African-Asian continent (i.e., from the monsoon to the
780 "deserts" on the left and from the "deserts" to the monsoon on the right).